

The Ui Group and Late Riphean Sills in the Uchur–Maya Area: Isotope and Paleomagnetic Data and the Problem of the Rodinia Supercontinent

V. E. Pavlov*, Y. Gallet**, P. Yu. Petrov***, D. Z. Zhuravlev****, and A. V. Shatsillo*

**Schmidt Joint Institute of Physics of the Earth, Russian Academy of Sciences,
Bol'shaya Gruzinskaya ul. 10, Moscow, 123810 Russia*

***Paris Institute of Physics of the Earth, National Research Center, 4, Place Jussieu, Paris, 75252 France*

****Geological Institute (GIN), Russian Academy of Sciences, Pyzhevskii per. 7, Moscow, 109017 Russia*

*****Institute of the Geology of Ore Deposits, Petrography, Mineralogy, and Geochemistry (IGEM),
Russian Academy of Sciences, Staromonetnyi per. 35, Moscow, 109017 Russia*

Received September 25, 2000

Abstract—Detailed paleomagnetic studies of the Ui Group of sedimentary rocks and Late Riphean basic sills from the Yudoma–Maya zone of the Uchur–Maya area have been performed. The Sm–Nd and K–Ar radiometric ages of the sills were determined. A high-confidence paleomagnetic pole was obtained for the Siberian Craton, corresponding to an age of 942 ± 19 Ma. Along with the poles previously obtained for the Kerpyl' and Lakhanda groups of the Uchur–Maya area, the new pole makes up a segment of the apparent pole wander path describing the paleogeographic position and drift of the Siberian Craton during the time interval between 1070–1030 and 1000–950 Ma ago. A comparison of the new segment and the respective paths for Laurentia and East Gondwana suggests that these cratons might have been parts of one supercontinent only if the generally accepted option of the polarity of Precambrian paleomagnetic directions is revised for Laurentia (and East Gondwana) or Siberia. The use of the polarities of the paleomagnetic directions proposed in [31, 37, 39] suggests that the paleomagnetic poles of the reviewed cratons fall into the same region of the globe after the matching of East Gondwana with Laurentia as in the classical configuration of Rodinia and after connecting the SSW portion of Siberia with the northern part of Laurentia. In such a configuration, the respective segments of the apparent polar wander paths for Siberia and Laurentia virtually repeat one another, this supporting the view that these cratons belonged to the same supercontinent during the Middle and Late Proterozoic.

INTRODUCTION

Despite the generally accepted hypothesis of the Late Proterozoic Rodinia supercontinent, a rigorous examination of the data available suggests that the mere fact of this continent's existence cannot currently be taken as an established fact. A comparison between the Meso- and Neoproterozoic segments of the apparent polar wander paths of the ancient cratonic blocks, interpreted in [22, 26, 42] as parts of this supercontinent, is one of the most reliable ways of testing this hypothesis. If the cratons reviewed were indeed parts of Rodinia, their apparent polar wander paths for the period of 1100–750 Ma must coincide after their being restored to the configuration in which they participated in the structure of the supercontinent.

Powell *et al.* [35] demonstrated in 1993 that the Laurentia and East Gondwana apparent polar wander paths indeed coincided to a first approximation within the Rodinia configuration suggested by Hoffman, Dalziel, and Moors [22, 26, 30]. Similar research will have to be carried out to test the hypothesis on Siberia being a part of Rodinia and to determine the mutual positions of Siberia and Laurentia within the framework of one

supercontinent. For this, we must have at least several reliably dated paleomagnetic poles for Siberia, corresponding to the assumed time of Rodinia's existence. Two of these poles are already known. One of them (dated 1045 ± 20 Ma) was obtained using rocks of the Malga Formation in the Uchur–Maya area [2, 10, 25], the other corresponding in the time to the accumulation or the lower rocks of the Lakhanda Group (1025 ± 40 Ma) in the same part of the Siberian Craton [2, 11]. A third pole, which was obtained previously for Late Riphean sills of the Uchur–Maya area and their host rocks, can be used as a third reference pole for constructing an apparent polar wander path. However, firstly, their dating has not yet been reliably substantiated, and secondly, the paleomagnetic directions used were obtained by means of laboratory procedures that, according to the latest requirements, are not sufficient for the precise determination of natural remanent magnetization components.

Our study included isotope dating of the sills mentioned above and control measurements that allowed use to estimate the accuracy of the previous paleomagnetic determinations. We obtained the new data simul-

taneously, which allowed us to refine the position of the paleomagnetic pole for the Late Riphean Ust'-Kirba Formation in the Uchur-Maya area. These data were used to test the hypothesis of a Late Proterozoic supercontinent.

BRIEF GEOLOGICAL DESCRIPTION OF THE STUDY OBJECTS

The Uchur-Maya region (Fig. 1) consists of the Uchur-Maya plate, which is a part of the Siberian craton, and the Yudoma-Maya zone, which is a junction zone between the Siberian Craton and the Verkhoyansk-Chukchi Mesozoic fold area [14]. It is important that the Nel'kan suture that separates the Uchur-Maya plate and the Yudoma-Maya zone practically does not extend into the crystalline basement of the zone, which represents the direct continuation of the basement of the Siberian Craton, and is essentially confined to its sedimentary cover [12, 15, 16]. This circumstance justifies the use of the paleomagnetic poles of the Yudoma-Maya zone for the whole of the Siberian Craton or at least for its Aldan block. The feasibility of using the paleomagnetic poles of the Yudoma-Maya zone for constructing apparent polar wander paths is also supported by the results of earlier paleomagnetic studies [8], which precluded any significant motions of the inner blocks of the Yudoma-Maya zone relative to the Siberian Platform. Because the geological structure of the Uchur-Maya region was described earlier [1, 14], we shall restrict our selves to that which is directly related to the objects of our study.

The basically homogeneous clastic rocks of the Ui Group, which encloses the Late Proterozoic sills we examined, crowns the Riphean sequence of the Uchur-Maya region (Fig. 1). These rocks rest, without any obvious evidence of a stratigraphic unconformity, on the carbonate deposits of the Late Riphean Lakhanda Group, their top being truncated by a large regional pre-Yudoma erosion surface. The thickness of the Ui Group varies from a few hundred meters within the Uchur-Maya plate to a few kilometers in the Yudoma-Maya zone, which is controlled not only by the thickness of the sediments that accumulated there but also by the depth of the previously mentioned erosion. The Ui Group is subdivided, according to [14], in terms of the lithology of its rocks, into two regionally developed formations, viz., the lower Kandyk Fm. and the upper Ust'-Kirba Fm, which are connected with each other by a gradual transition.

The Kandyk Formation consists of interbedded gray and greenish gray subarkose sandstones and silty argillites. The sandstone layers show a parallel gradation bedding and numerous erosion surfaces at their bases and washout channel casts. Thin gradational structures of suspension storm-related and turbidite sedimentation are characteristic of the silty argillite. The proportion of a pelitic grain-size fraction (argillite) is insignificant as compared to the bulk of the sediment; thin lay-

ers of gravel and shingle occur at some levels of the sequence. The thickness of the formation increases eastward away from the margin of the Uchur-Maya plate toward the trough of the Yudoma-Maya zone.

The Ust'-Kirba Formation is a monotonous alternation of gray, greenish, and, locally, variegated flaggy siltstones and mudstones with the subordinate beds of light gray quartz and subarkose sandstone. Carbonate occurs at some levels of the deposits. Nearly all rocks show a thin parallel usually gradational, bedding; distinctly pronounced erosional textures occur as exceptions. The Ust'-Kirba deposits have been preserved in the contemporary structure of the area almost exclusively within the Yudoma-Maya zone, where their thickness varies from 200 to 1500 m.

Taken as a whole, the data available [6] suggests that the Riphean sedimentary rocks of the Uchur-Maya region have undergone merely the initial stages of depth epigenesis. This is expressed in a change of the clay mineral composition in the silty argillite and in the occasional evidences of interpenetration microstructures at the contacts between the sandstone grains.

The Ui rocks were found to be monoclinial in almost all the examined outcrops with some local variations of their dips and strikes, the dip angles varying from 15 to 30°C. The only exceptions are local sharp folds and flexures up to 10 m high that occur occasionally in some narrow, usually fault-related zones. The original horizontal bedding of the Riphean sedimentary rocks was violated only in the Latest Mesozoic, simultaneous with a folding episode in the Verkhoyansk-Chukchi region [14].

Late Proterozoic subvolcanic bodies, such as gabbro-diorite sills and dikes, ranging from a few meters to a few hundred meters in width, are rather common in the Yudoma-Maya zone. The sills are concordant with the host rocks. There are distinct indications of the sills' thermal action upon the enclosing rocks, which can be observed only in narrow (1-2 m wide) exomorphic zones. The exomorphic formations in the Kandyk Fm. rocks are represented by bedded and mottled hornfelses formed after the aleuropelitic rocks and containing finely disseminated ore minerals and abundant chlorite-sericite pseudomorphs after cordierite, suggesting the effect of high-temperature contact metamorphism. All discernible evidence of the sills' thermal effect upon the host rocks vanishes rapidly away from the sills.

The relative dating of the sills and their host rocks was a fairly easy task. On the one hand, the sills are confined to the Middle and Upper Riphean rocks up to the lower Kandyk ones. On the other hand, the pebbles derived from these sills were found at the base of the upper Kandyk deposits [14]. These data suggest that the sills had been intruded either at the end of the early Kandyk time or at the boundary between early and late Kandyk time.

As for the isotope ages of the examined sills and their host rocks, the data were limited until recently by a few datings of the glauconite from the basal and mid-

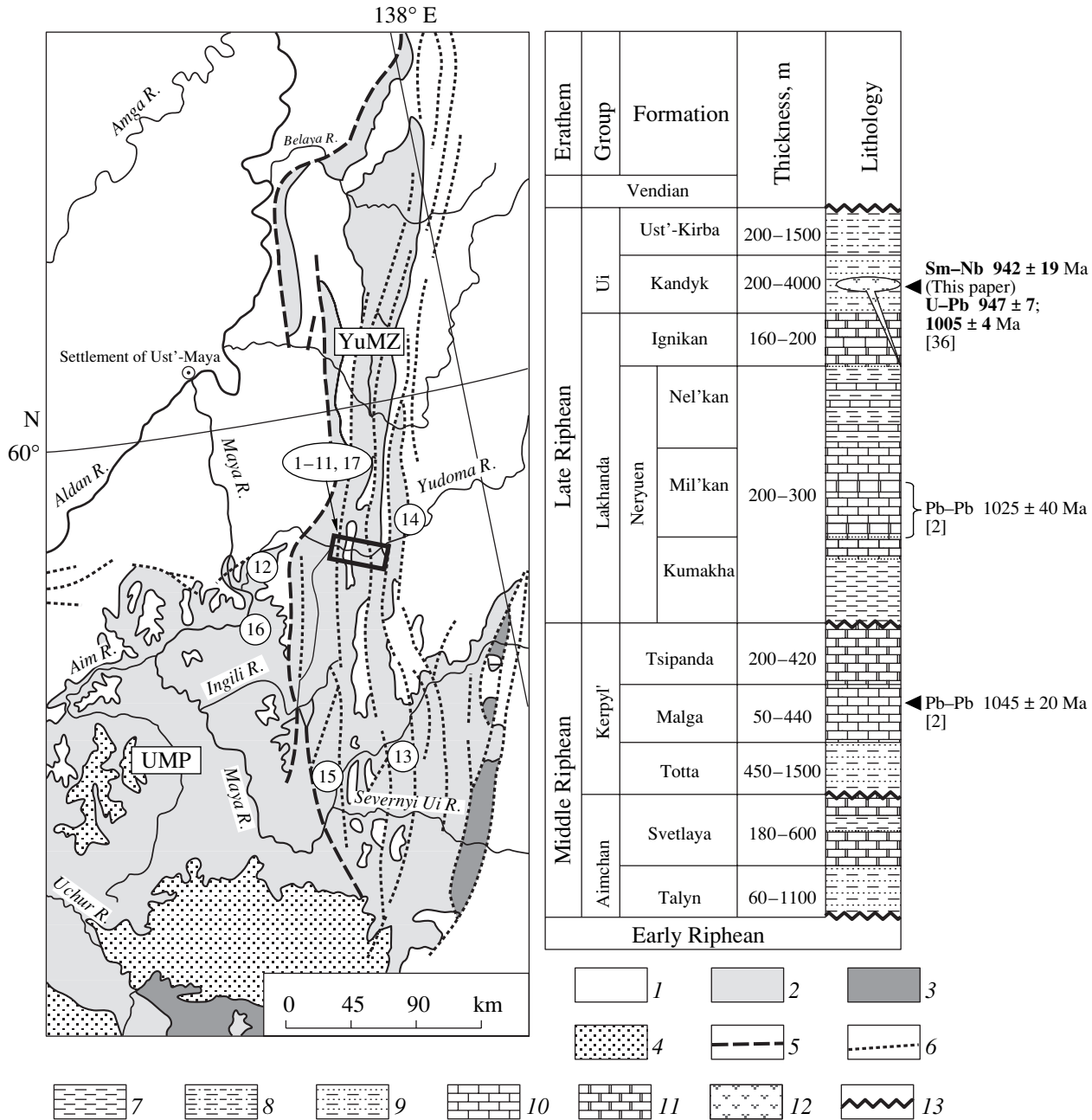


Fig. 1. Geological setting of the study objects and the composite stratigraphic section of the Middle and Upper Riphean deposits in the Uchur–Maya area. Map: (1) Phanerozoic rocks; (2) Riphean and Vendian (Yudomian) rocks; (3) pre-Riphean volcano-plutonic complex; (4) crystalline basement (Archean and Early Proterozoic); (5) main faults (Nel'kan marginal suture); (6) subordinate faults of the Yudoma–Maya zone. Composite stratigraphic section: (7) mudstone; (8) siltstone; (9) sandstone, siltstone, and mudstone; (10) limestone; (11) dolomite; (12) diabase sills; (13) major stratigraphic hiatuses. Numbers on the map denote the sites of examined outcrops: Late Proterozoic sills: 1—P; 2—C; 3—JU; 4—S; 5—I; 6—110; 7—G; K—contact zones; Kandyk Fm. rocks, sites: 9—1998; 10—108; 11—113; 12—125; 16—Bol'shoi Kandyk R. mouth; outcrops of Ust'-Kirba Fm. rocks: 13—Kaval'kan; 14—Kirytyga; 15—Severnyi Ui; 17—Tyallakh. YuMZ—Yudoma–Maya zone; UMP—Uchur–Maya plate.

dle levels of the Kandyk Formation (760 and 700 Ma, respectively) [14]. These data basically agree with the K/Ar datings of other Riphean rocks from the Uchur–Maya area, which yielded a regular series of age values increasing down the sequence. We should note, how-

ever, that the glauconite age determinations were done over a quarter century ago using procedures that did not meet modern requirements for age determinations. The need for new datings corresponding to the modern level of geochronologic studies was evident.

NEW RESULTS OF OUR ISOTOPE STUDY

Samples for our study were collected from the sills outcropping on the Yudoma River's left bank approximately 8 km south of the Mouth of the Pukhanil River. The isotope studies were performed at the Institute of the Geology of Ore Deposits, Petrography, Mineralogy, and Geochemistry, Russian Academy of Sciences in accord with the technique described in [5]. A mixed $^{149}\text{Sm} + ^{150}\text{Nd}$ spike was added to every specimen of 100–200 g for our Sm–Nd isotope analyses. The specimens were decomposed in a mixture of nitric and hydrofluoric acids for two days at a temperature of 100°C. Nd and Sm were separated in the following two stages: firstly, all rare-earth elements were separated from the major components using a DOWEX 50*8 cationite, and then Sm and Nd were separated using a di(2-ethylhexine)orthophosphoric acid applied to an inert solid phthoroplast-3 carrier. The blank values were 0.3 ng Nd and 0.1 ng Sm, which were negligible compared to the abundances of these elements in the specimen.

The mass spectrometry of Sm and Nd was performed using an MI-1320 mass spectrometer, single-beam measurements and a two-filament (2^*Re) ion source. The isotope ratios were normalized for $^{146}\text{Nd}/^{144}\text{Nd} = 0.7219$. The parallel measurements using a La Jolla reference sample yielded an average value of $^{143}\text{Nd}/^{144}\text{Nd} = 0.511842 \pm 20$ ($N = 10$, t^*_{pop}), which coincided within the uncertainty interval with the best value for this specimen. Therefore, no corrections were applied to the results presented in Table 1. The error of the $^{147}\text{Sm}/^{144}\text{Nd}$ ratio determination was estimated from the results of analyzing a reference BCR-1 rock at 0.2% rel.

The following errors were adopted along the axes of the isochrone diagram for computing the isochrone parameters: 0.2% rel. along the $^{147}\text{Sm}/^{144}\text{Nd}$ axis and the maximum error of the convergence values for the individual analysis data along the $^{143}\text{Nd}/^{144}\text{Nd}$ axis. This error was ± 0.000022 for the WR specimen and ± 0.000020 for the minerals. The isochrone parameters were computed using York's [43] technique, and the initial value, viz., $\epsilon\text{Nd}(T)$, using the method of Fletcher and Rosman [24]. The isochrone parameter uncertainties agreed within two standard deviations. The results of our Sm–Nd analyses of the rocks and minerals are listed in Table 1.

A regression line with the following parameters approximated the data points in the isochrone diagram

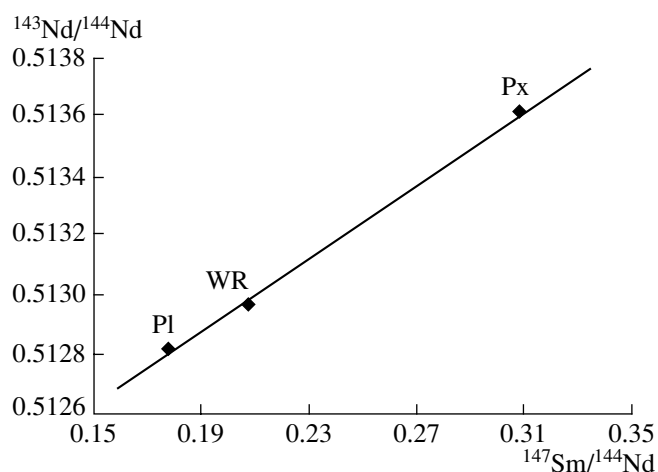


Fig. 2. Isochrone diagram showing the results of Sm–Nd isotope analysis.

(Fig. 2): $T = 942 \pm 19$ Ma, $\epsilon\text{Nd}(T) = +5.5 \pm 0.3$, and $\text{MSWD} = 1.1$. This age value obviously corresponds, taking the good linearity of the isochrone into consideration, to the time of the last isotope equilibrium between the rock minerals. This means that they date the respective magmatic event, since the examined minerals were found by our preliminary petrographic examination of the rocks in thin sections to be primarily magmatic and bearing no evidence of secondary alterations.

However, this result was found to be considerably different from the previously adopted ages of the examined rocks. Therefore, we attempted to confirm the sill's age using an independent isotope method. For this purpose, we made a K/Ar analysis of a primary magmatic hornblende separated from the rocks that compose the sill. This analysis was made using a technique described in detail in [18]. The isotope ratios obtained corresponded to the hornblende age of 970 ± 100 Ma. The low accuracy of the K/Ar age determination was caused by a low ($\sim 0.08\%$) potassium content in the mineral and by the extremely small specimen of the mineral that could be separated from the available sample. Nonetheless, the good agreement of the results obtained by both the Sm/Nd and K/Ar determinations confirmed the reliability of our Sm/Nd dating. The more so, our isotope age value, although being somewhat lower, sufficiently well corresponds, on the

Table 1. Mass-spectrometry results

No.	Study object	Sm	Nd	$^{147}\text{Sm}/^{144}\text{Nd}$	$^{143}\text{Nd}/^{144}\text{Nd}$
1	Whole-rock	2.46	7.20	0.0268	0.512973 ± 22
2	Plagioclase	0.721	2.45	0.1779	0.512807 ± 10
3	Pyroxene	1.19	2.34	0.3078	0.513608 ± 11

Note: See text for the explanations.

whole, to the results reported in [36]: 947 ± 7 and 1005 ± 4 Ma. These data were obtained using a U-Pb method for other sills from the Late Riphean rocks of the Uchur-Maya, using baddeleyite. We cannot suggest any substantiated explanation for the small difference between our age values and those separated in [36]. This difference might have been caused by an unnoticed systematic error in one of the experiments or may reflect some real differences between the ages of the sills examined by the present writers and our colleagues.

To conclude, the data available suggest that the Late Proterozoic sills of the Uchur–Maya area and their host rocks of the Kandyk Formation were formed during the time interval of 940–1000 Ma.

PALEOMAGNETIC MEASUREMENTS

Methods and Objects of Study

Our paleomagnetic study included the reexamination of the samples collected in the late 1980s (the remaining samples) using the modern equipment and procedures, the verification of previously obtained and partly published data [9], and the analysis of new samples collected during a 1998 field season. Our objects of study were Late Proterozoic sills and their exocontact zones, as well as the Kandyk and Ust'-Kirba Fm. sedimentary rocks outcropping in the valleys of the Maya and Yudoma rivers and their tributaries (Table 2, Fig. 1).

In the course of this study, rocks of the Kandyk Formation were examined in a stratigraphic section near the Mouth of the Bol'shoi Kandyk River (Site 16, Fig. 1), as well as in the outcrops of the Suordanakh tract (sites 9–11) and on the left bank of the Yudoma River valley 21 km upstream from its mouth (Site 12). Outcrops 9–11 were a few hundred meters away from the nearest sills and do not show any evidence of their effects. Outcrops 12 and 16 were located several dozens of kilometers from the nearest Late Proterozoic magnetic bodies.

The samples of Late Proterozoic sills and their exocontact zones (Outcrops 1–8) were collected within the Sourdanakh tract (lower reaches of the Yudoma River 7–8 km downstream from the Mouth of the Pukhanil River mouth).

The rocks of the Ust'-Kirba Formation were examined in the following outcrops: (1) Kaval'kan (Site 13) located on the left bank of the Maya River approximately 15 km downstream from the settlement of Kaval'kan; (2) Severnyi Ui (Site 15) located on the right bank of the Maya River 15 km upstream from the mouth of the Severnyi Ui River; (3) Kyry-Ytyga (Site 14) located on the right bank of the Yudoma River downstream of the mouth of the Kyry-Ytyga River; and (4) Tyallakh (Site 17) represented by low cliffs on the right bank of the Yudoma River downstream of the Mouth of the Tyallakh River.

Earlier [9], when processing sample collections of the late 1980s, we used the following technique in the process of the laboratory studies. A pilot collection was arbitrarily selected for every outcrop, which usually made up 15–20% of the total number of the specimens. The pilot collection was then subjected to a thorough demagnetization, and the results of the latter were used as a basis for choosing an optimum magnetic cleaning regime; i.e., the temperature or the magnitude of the alternating magnetic field, which, as it was conceived, left only a characteristic component. Then, the whole collection was cleaned under some chosen optimum conditions.

The choice of this technique was determined at that time by the absence of highly sensitive and highly productive instruments, the low quality of demagnetization equipment, the limited access to computers, and a lack of computer programmes for using the modern methods of a component analysis.

It is evident that the instruments and methods that were used could provide well-grounded results only in the case of very homogeneous collections with a simple component composition of magnetization and at relatively low releasing temperatures, which spoil the experiment. The results of the detailed cleaning of pilot specimens provided some grounds to believe that the above conditions were basically satisfied, although the results obtained were insufficient to state this with confidence. Moreover, one had to bear in mind that only some part of the pilot collection could be actually used for analyzing the magnetization component composition, viz., that which did not undergo any significant temperature alterations or superimposed magnetic biasing in the course of magnetic cleaning. This considerably decreased the representativeness of the results of detailed demagnetization. Recently, the possibility appeared to undertake duplicate measurements using some samples from old collections at a considerably higher level and to estimate the reliability of the results we obtained earlier from the positions of the modern requirements.

The laboratory paleomagnetic studies and the primary processing of their results were carried out in the Paleomagnetic laboratories of the IFZ RAN (Joint Institute of Physics of the Earth, Russian Academy of Sciences), Moscow, and in the Paris Institute of Physics of the Earth by a conventional method [17, 20, 27, 44] and using modern technique and software achievements [23, 28, 29, 41].

All samples were subject to thermal cleaning, which was carried out, in most cases, at temperatures of 685–690°C. The number of cleaning steps was usually not more than 11–12; in some cases, it was greater. Special nonmagnetic furnaces with a noncompensated field intensity not exceeding 5–10 nT were used for the demagnetization. Remanent magnetization was measured using cryogenic 2G Enterprises and CTF magnetometers. All laboratory procedures were performed in

Table 2. Paleomagnetic data and poles obtained for Late Proterozoic sills and for Kandyk and Ust'-Kirba fm. rocks

Object	Object/Coordinates, deg	Processing	N	Geographic coordinate system, deg				Stratigraphic coordinate system, deg				γ/γ _c	
				D	I	K	α ₉₅	D	I	K C	α ₉₅		
Sills and their baked contacts	1. Sill P/ λ = 136.4; φ = 59.4	I	28	156	36	25.1	5.1	135	34	25.6	5.0	8.2/8.6	
		II	19	165.1	39.5	27.4	6.5	139.4	41.5	24.3	6.9		
	2. Sill C/ λ = 136.4; φ = 59.4	I	22	161	40	52.3	4.0	140	35	52.3	4.0	4.9/5.9	
		II	20	158.2	44.2	62.3	4.2	134.8	37.6	62.3	4.2		
	3. Sill JU/ λ = 136.4; φ = 59.4	I	16	160	39	30.5	6.0	137	36	30.7	6.0	6.2/9.6	
		II	10	153.5	35.5	62.3	6.2	134.5	30.2	59.4	6.3		
	4. Sill S/ λ = 136.4; φ = 59.4	I	21	160	38	114.9	2.8	141	33	114.9	2.8	2.9/4.4	
		II	17	159.4	40.4	112.7	3.4	138.4	35.0	112.3	3.4		
	5. Sill I/ λ = 136.4; φ = 59.4	I	14	157	40	33.1	6.5	135	36	33.6	6.5	7.0/8.6	
		II	12	150.7	35.2	72.4	5.1	133.2	29.2	74.9	5.0		
	6. Sill 110/ λ = 136.4; φ = 59.4	I	11	157	49	32.1	8.2	132	37	34.2	7.2	12.3/12.1	
		II	12	165.1	38.6	20.2	9.9	145.5	31.7	21.7	9.5		
	7. Sill G/ λ = 136.2; φ = 59.4	I	7	152	41	7.5	19.2	138	27	7.5	19.2		
		II				No new data available							
	8. Contact K/ λ = 136.4; φ = 59.4	I	21	159	42	46.7	4.1	137	34	47.8	4.0	1.7/7.2	
		II	16	160	40.4	56.9	4.9	138.8	33.2	41.4	5.8		
Kandyk Fm. siltstones and sandstones	9. Site 1998/ λ = 136.4; φ = 59.4	I		No old data available									
		II	10	162.8	51.6	22.0	8.0	129.3	47.0	28.4	7.0		
	10. Site 108/ λ = 136.4; φ = 59.4	I	7	165	44	62.3	6.7	141	37	73.0	6.2		
		II		No new data available									
	11. Site 113/ λ = 136.4; φ = 59.4	I	3	121	12	52.8	18.0	147	36	88.5	15.2		
		II		No new data available									
12. Site 125/ λ = 135.3; φ = 59.3	I	10	140	53	6.0	18.1	143	42	6.1	18.1			
	II		No new data available										
Average for objects of Kandyk age		I	11	153.0	40.2	31.2	8.3	138.7	35.2	266.7	2.8	1.6/5.1	
		II	8	159.2	40.8	149.9	4.5	136.9	35.8	125.3	5.0		
Average pole for objects of Kandyk age		II	8	Φ = -3.1; Λ = 176.5; K = 167.3; A₉₅ = 4.3									
Ust'-Kirba Fm. siltstones and clayey siltstones	13. Kaval'kan λ = 136.7; φ = 58.2	I	24	140.4	28.4	20.1	6.4	130.5	37.0	19.7	6.4	8.9/12.4	
		II	8	136.8	43.5	57.6	7.4	125.9	29.0	52.7	7.7		
	14. Kury-Ytyga λ = 137.1; φ = 59.4	I	31	138.3	26.0	19.5	5.7	135.4	16.7	20.2	5.6	9.1/12.8	
		II	8/12	140.8	26.6	44.0	5.2	139.5	20.3	43.2	5.2		
	15. Severnyi Ui λ = 136.3; φ = 57.9	I		Characteristic component direction could not be determined									
	II	5/2	140.8	26.6	44.0	5.2	139.5	20.3	43.2	5.2			
Average for Ust'-Kirba Fm.		I	2	139.3	27.2			133.2	26.9				
		II	3	140.9	35.6	80.7	13.8	133.0	26.1	105.5	12.1		
Average pole for Ust'-Kirba Fm		II	3	Φ = -8.1; Λ = 182.6; K = 142.1; A₉₅ = 10.4									

Note: N is the number of specimens from an outcrop or the number of outcrops for an average value. The entries 8/12 and 5/2 mean 8 (5) "final directions" and 12 (2) large circles; D, I, C, and α₉₅ are Fisher distribution parameters; is the angular distance between the compared vectors; γ_c is the critical angle. Processing: I magnetic cleaning at a given temperature chosen from the results of the detailed demagnetization of the pilot collection; II detailed thermal demagnetization of every specimen with subsequent component computation using the PCA technique; Φ and Λ are the latitude and longitude of the average paleomagnetic pole; A₉₅ is a confidence circle radius; K is grouping density; φ and λ are the latitude and longitude.

a compartment screened from the external magnetic field. Enkin's [23] software package was used to process the measurement results. The PCA technique [27] was used for separating the magnetization components. It was accepted, in doing this, that a rectilinear segment of a Zijdeveld diagram, supported by at least 3–4 data points, corresponded to the magnetization component.

The value of the natural remanent magnetization in the examined sills varied within 1–15 A/m; it was $0.5\text{--}5 \times 10^{-3}$ A/m in the Kandyk Fm. rocks and $1\text{--}12 \times 10^{-3}$ A/m in the Ust'-Kirba Fm. rocks. Magnetic susceptibility was usually $10\text{--}30 \times 10^{-3}$ SI in the sills, $30\text{--}70 \times 10^{-6}$ SI in the Kandyk rocks, and $15\text{--}110 \times 10^{-6}$ SI in the Ust'-Kirba rocks.

Magnetic Cleanings

Sills and their contact zones. The detailed cleaning results confirmed the conclusion made in [9] on the two-component composition of the natural remanent magnetization of the rocks of the sills and their baked contacts (Fig. 3). However, the mass cleanings demonstrated, contrary to the results of the pilot collection examinations, that a less stable component may, in a number of cases, possess a wider spectrum of releasing temperatures than had been presumed previously. The maximum releasing temperatures of this component, which is close to the present-day magnetic field, can be as high as 500–520°C. The characteristic component (ChRM), whose carrier is magnetite, as had been shown in publication [9], or compositionally similar titanomagnetite, was usually destroyed within the temperature interval of 420–580°C (Figs. 3a, 3c). The majority of the magnetization of specimens from exocontact zones was destroyed within the temperature range of 320–360°C (Fig. 3b), similar to the Kandyk rock samples collected at a considerable (hundreds of meters) distance from the intrusive contacts (Fig. 3e). The component destroyed in this case had the same orientation as the characteristic components in other samples from the exocontact zones and sills.

Kandyk Formation. The Sandstones and siltstones from the Maya River valley should only one magnetization component, close in its orientation to the contemporary magnetic field and, probably, owing its origin to the partial oxidation of the pyrite abundant in these rocks [7].

In Zijdeveld diagrams based on the cleaning results of the siltstones and sandstones from the Suordanakh tract area (Fig. 3, E), a rectilinear segment corresponding to a magnetization component that vanishes within a temperature interval of 300–360°C was distinguished confidently, in addition to a low-temperature component close to the contemporary magnetic field. This component seems to be associated with magnetic iron sulfides, possibly with pyrrhotite. The magnetization that remained in these specimens after cleaning at a temperature of 380–400°C accounted for not more than

15–20% of the original value and vanished completely at a temperature of 470–520°C. This magnetization was found, on the average, have the same orientation as the "pyrrhotite" component (although with a considerably greater scatter) and might have been caused by small, single-domain magnetite grains close in size to a transition into the superparamagnetic state.

Ust'-Kirba Formation. The examined rocks of the Ust'-Kirba Formation can be subdivided, based on their behavior in the course of the temperature magnetic cleaning, into four groups. The first group includes the samples, usually of red color, collected predominantly from the Kyry-Ytyga and Kaval'kan outcrops. Two magnetization components were clearly distinguished in them (Fig. 3, plates d, f, g): a less stable component that was destroyed completely at heating to 420–620°C, and a characteristic one whose maximum releasing temperatures were close to a hematite Curie point (in some samples, to a magnetite Curie point). The less stable component was distinguished by its steep inclination (usually 70°), and its orientation close to the direction of the Mesozoic–Cenozoic magnetic field of the Earth in the study area and was inferred to be of the same age.

The second group includes the samples of greenish and grayish green rocks collected from the Kyry-Ytyga and Sevenyi Ui outcrops. The character of changes of the natural remanent magnetization vector in these rocks unambiguously suggested the presence of two magnetization components in them, viz., a less stable one and a characteristic one. However, contrary to the samples of the first group, chaotic changes of the natural remanent magnetization vector began in these specimens in the temperature range of 420–450°C. This seems to have been related to the origin of new magnetic minerals, which precluded the direct determination of a characteristic component. Nonetheless, the projections of the natural remanent magnetization vectors of these specimens onto a stereogram (Fig. 4) formed large circles in the process of cleaning, which, along with the other data, can be used to compute the average direction of the characteristic magnetization.

The third group includes samples collected mainly from the Tyallakh outcrop, whose natural remanent magnetization vectors behaved chaotically in the process of cleaning. The samples of the fourth group were distinguished by the lack of any components, except for the Recent (Cretaceous–Cenozoic) one. This group consisted mainly of the samples collected from the Severnyi Ui outcrop.

A Analysis of Vector Distributions

Sills, exocontact zones, and the Kandyk Formation. Table 2 lists the paleomagnetic directions for a number of the examined outcrops both obtained earlier by us from the results of the sample cleanings according to a previously chosen optimum regime and new

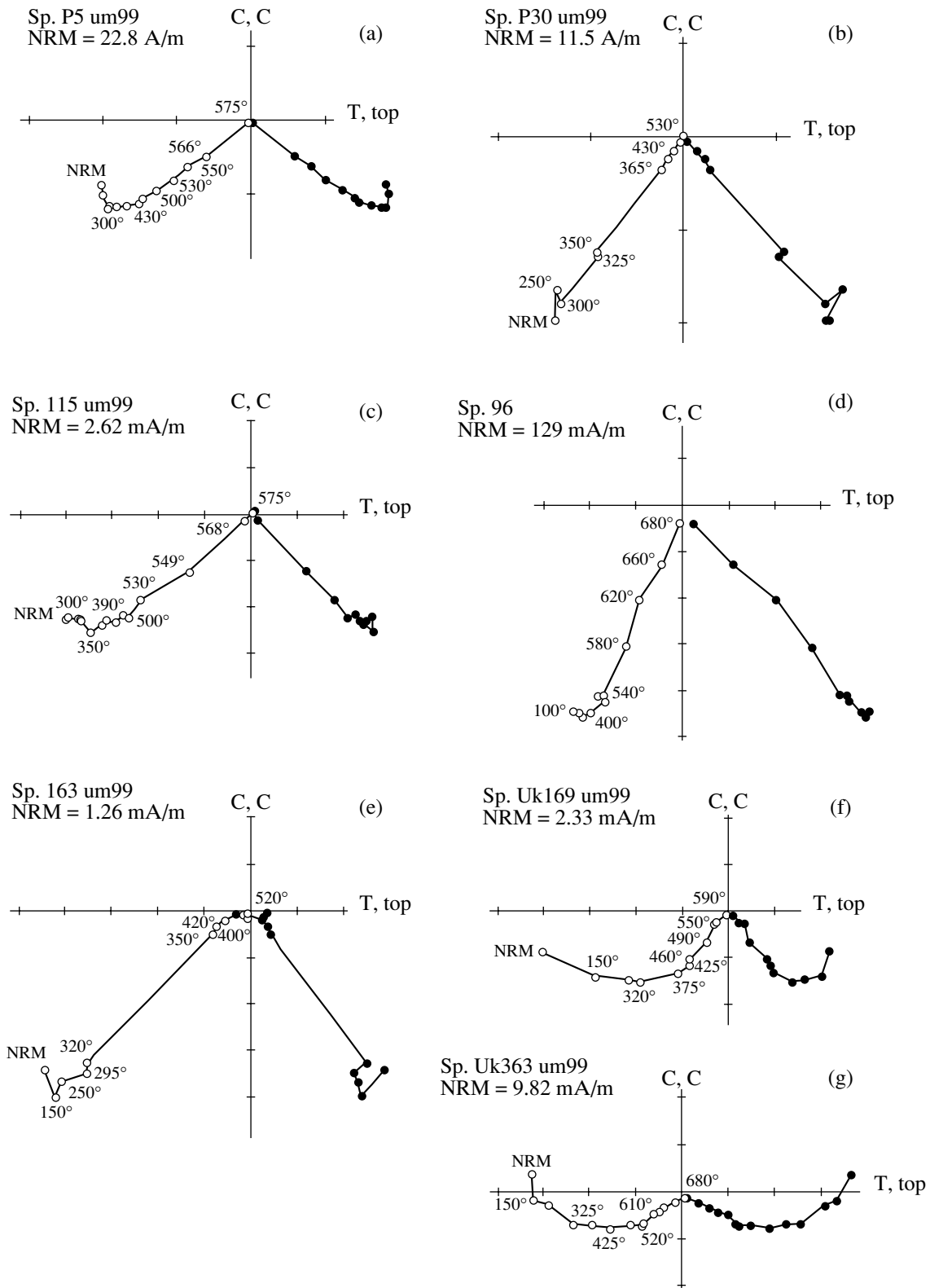


Fig. 3. Typical Zijderveld diagrams for the examined rocks. (a, c) Sills; (b) baked exocontact rocks; (e) Kandyk Fm. rocks located farther than 100 m from the nearest sill; (d, f, g) are Ust'-Kirba rocks from Sites 14, 13, and 15, respectively; solid circles are the projections of the natural remanent magnetization vectors on the horizontal plane; open circles—same, on the vertical plane. The diagrams are given in the stratigraphic coordinate system.

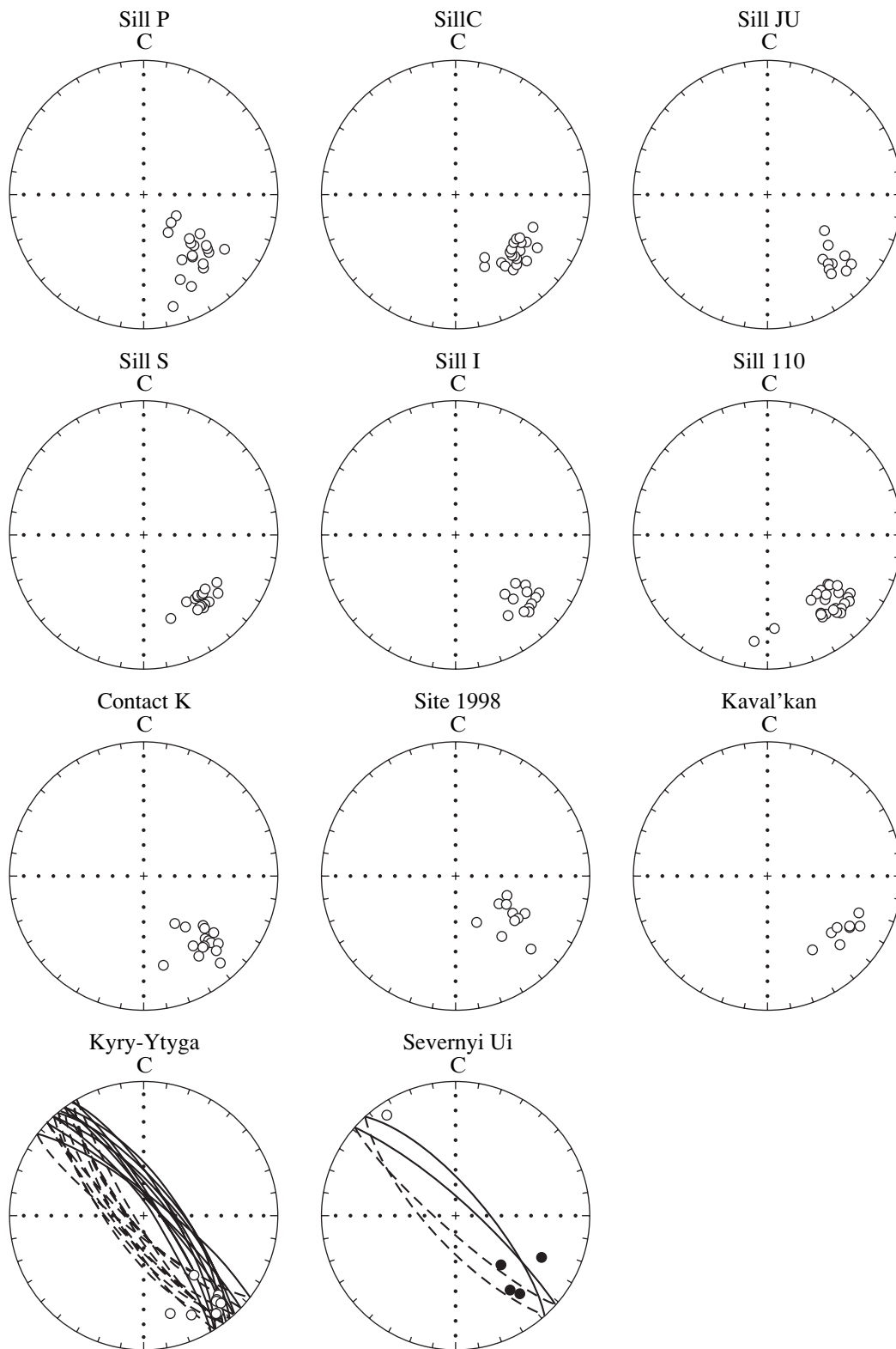


Fig. 4. Distribution of the characteristic magnetization vectors in the examined outcrops. Solid circles solid are the projections of the characteristic component vectors onto the lower hemisphere; open circles, same for the upper hemisphere; solid (dashed) lines in the diagrams show the projections of the great circles on the lower (upper) hemispheres. The stereograms have been reduced to the stratigraphic coordinate system.

Table 3. Paleomagnetic poles of Siberia, Laurentia, and East Gondwana

N*	Age, Ma	Paleomagnetic poles				Reference	Polarity option		
		Φ	Λ	N	A ₉₅		1	2	3
SIBERIA									
1	1035 ± 20	-22.5	230.4	4	2.5	[10]	N	N	S
2	1000–1030	-13.3	203.2	8	10.7	[11]			
3	950–1000	-3.1	176.7	3	4.3	This paper			
4	950(?)	-8.1	182.6		10.4				
5	V	-33	117	–	–	Gurevich, referred to in [39]			
6	V– ϵ_1	-38	165	–	–		[33]		
7	ϵ_1	-45	159	–	–				
8	$\epsilon_{1,2}$	-36	140	–	–				
LAURENTIA									
1	1100–1110	44.8	192.2	3	27.3	[42]	N	S	N
2	1085–1100	32.9	179.7	6	7.4				
3	1050–1075	24.3	176.8	4	12.0				
4	1000–1020	9.2	164.6	6	16.1				
5	960–990	-23.1	147.8	3	26.8				
6	830 ± 50	10.5	148	2	–	[35]			
7	810 ± 40	-11	144	2	–				
8	780 ± 5	-5.5	138	4	6.1				
9	725 ± 5	5.9	162.4	2	–				
10	580 ± 20	-43.5	124.5	3	7.6				
11	ϵ_1	-57.3	114.3	3	16.5				
EAST GONDWANA (poles are reduced to the present-day position of the Indian craton)									
1	1054 ± 14	61	22	1	12	[35]	N	S	N
2	720 ± 20	78.4	40	2	–				
3	V	55.6	226.0	5	9.2				
4	ϵ_1	37.0	208.5	9	11.2				
5	ϵ_{2-3}	12	206.5	5	14.8				

Note: N* are pole numbers for corresponding ancient cratons as given on the apparent polar wander path (Fig. 6, B); A, Λ are the latitude and longitude of the average paleomagnetic pole, deg; A₉₅ is the confidence circle radius of the average paleomagnetic pole; N is the number of poles used in averaging; Polarity options: 1 generally accepted (N means that the numbers given in the table correspond to the North Pole); 2 implying a change of magnetic direction polarity for Laurentia and East Gondwana (S means that the numbers given in the table correspond to the South Pole); 3 implying a change of the paleomagnetic direction polarity for Siberia). The dash means no data.

data on directions of magnetization characteristic components that were computed using the PCA technique from the results of the detailed cleanings. A comparison between the old and new data for all repeatedly examined sills and exocontact zones, obtained using the McFadden–McElhenny method [29] shows no significant differences between them.

We managed to duplicate our measurements only for 7 out of the 11 previously examined sites of the Kandyk rocks because of the small number of the samples available (Table 2). Nonetheless, the results of these measurements clearly indicate that our estimates of the characteristic magnetization directions obtained

previously do not differ in terms of statistical significance from the determinations performed using the modern methods and equipment. Hence, they can be used for further paleomagnetic solutions. The different number of objects, used for computing the average values, and their different structural settings may account for the obvious difference in the concentrations of the average directions for the old and new data.

Arguments in support of the point that the characteristic component distinguished in the sills and their contact zones does reflect the direction of the geomagnetic field during the Kandyk Fm. accumulation time were discussed in detail earlier [9]. They can be summarized

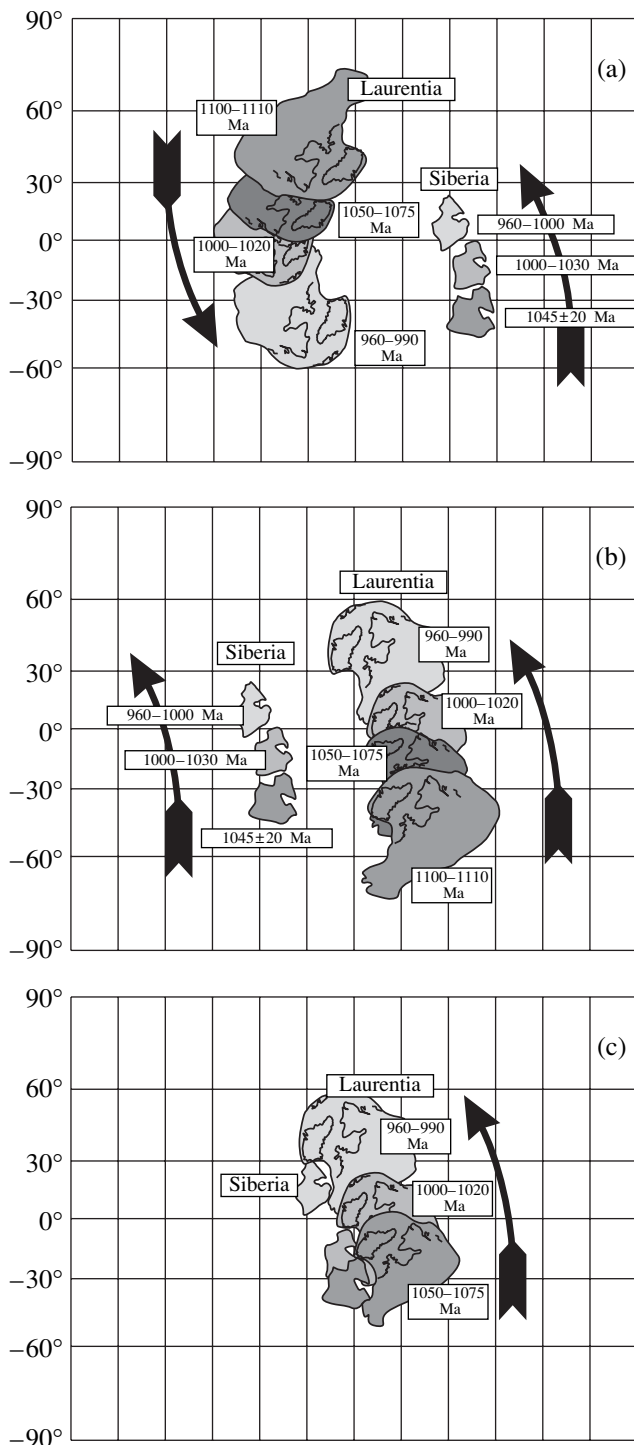


Fig. 5. Drift of Siberia and Laurentia 1100–950 Ma ago: (a) for the conventional polarity option [39, 42]; (b) for the polarity of the Proterozoic paleomagnetic directions after Park [31]; (c) the reconstruction of the relative positions of Siberia and Laurentia 1100–950 Ma ago.

as follows: (1) coincidence of paleomagnetic directions in objects separated by distances of tens of kilometers; (2) coincidence of paleomagnetic directions both in the heating and heated rocks; (3) coincidence of paleomag-

netic directions in coeval subvolcanic and sedimentary rocks; (4) coincidence of paleomagnetic directions associated with different magnetic minerals; (5) the pre-folding age of the distinguished component; (6) differences in the positions of the paleomagnetic pole corresponding to a distinguished component and the positions of the known younger paleomagnetic poles; (7) the thermoremanent nature of the characteristic magnetization of sills and exocontact zones.

The following facts support the last statement: (1) a coincidence between the characteristic component temperature spectra and the laboratory thermal remanent magnetization above the temperatures of 420–450°C; (2) the absence (under optical or electron microscope) of any minerals other than titanomagnetite and an approximately equal idiomorphism of clinopyroxene and titanomagnetite grains, indicating the magmatic origin of the latter; (3) the presence of chlorite–sericite pseudomorphs after cordierite indicating high-temperature heating of the exocontact rocks; (4) the characteristic granulation structure of titanomagnetite grains distinctly visible under electron microscope (such a structure originates, as shown in [2], due to the deep oxidation of titanomagnetite under high-temperature conditions); (5) the presence of titanomagnetite grains with an exsolution lattice where lamellae are ~0.5 μm wide. Such lamellae originate, according to [3], during high-temperature exsolution accompanied by oxidation at $T = 800^{\circ}\text{C}$.

Unfortunately, we could not perform a conglomerate test, because no pebbles produced by the erosion of the Late Riphean sills and occurring in the Uchur–Maya area were found in the outcrops we examined.

Since the data we obtained previously from a detailed magnetic cleaning and component analysis confirm the validity of the results reported previously [9], we may use the paleomagnetic pole presented in that paper for further reasoning. We admit, however, that using a magnetic pole based entirely on the data of the detailed magnetic cleaning (Table 2) would be methodically more correct.

Ust'-Kirba Formation. We managed to determine the direction of the ancient magnetization component in three of the four examined outcrops (Table 2). We had to use McFadden's [28] technique for computing the average directions in the Kyry-Ytyga and Severnyi Ui outcrops because of the small number of final directions obtained. This technique implies using large circles, i.e., the data that were obtained for the specimens of the second group (see the section *Magnetic Cleanings*).

The geological situation did not allow us to perform direct tests to time of the magnetization origin. Nonetheless, there is some indirect evidence indicating the primary nature of the selected component. These are: (1) the persistent orientation of the characteristic component (ChRM) over great distances; (2) a difference between the computed pole and the known younger

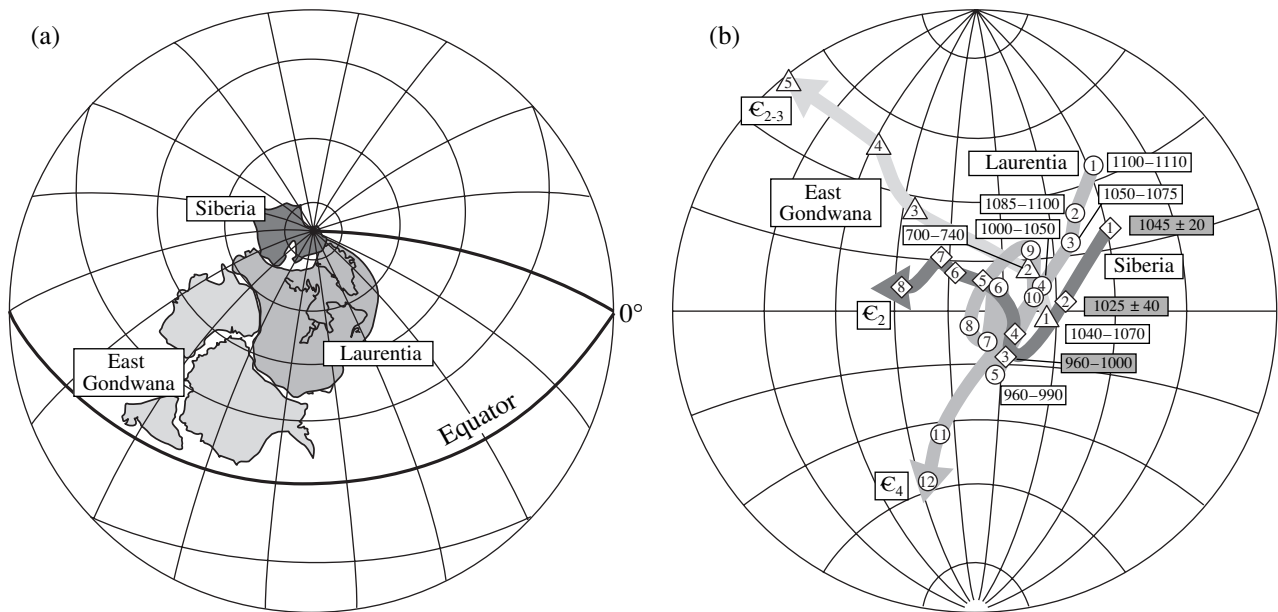


Fig. 6. (a) the a reconstruction of the relative positions of Siberia, Laurentia, and East Gondwana for 1100–950 Ma ago (shown relative to the present-day position of Laurentia); (b) apparent polar wander paths for Siberia, Laurentia, and East Gondwana. The APWP curves for Siberia and East Gondwana are rotated in accordance with Table 4. Numbers in rectangles show time intervals in Ma ago.

poles; and (3) the independence of the ChRM component orientation from the magnetic mineral association. The similarity between the resulting directions and the paleomagnetic directions in the magmatic rocks (sills) of an approximately similar age can also be taken as an argument in favor of the primary nature of the ChRM component in the Ust'-Kirba Fm. rocks.

DISCUSSION

The paleomagnetic poles we obtained in this study and the poles reported earlier [10, 11] for the rocks of the Malga Formation and the Lakhanda Group make up a sequence of paleomagnetic poles that describes the drift of the Siberian platform during the time interval of 1070–1030 to 1000–940 Ma ago. Practically all continental masses were amalgamated at that time, according to [22, 26], into one Rodinia supercontinent and must have experienced concordant motions, which were imprinted (in favorable instances) in the paleomagnetic record. If the hypothesis on Rodinia's existence is correct, then the apparent polar wander paths of the ancient continental blocks must coincide for the case when these blocks are matched in the same configuration in which they were amalgamated within the supercontinent [17]. Otherwise, taking into account possible uncertainties in the determinations of the poles' locations and ages, they must at least fall within the same region of the Earth's surface.

The results of this study allow us to compare the Siberian APWP with those for Laurentia and Gondwana. Sequences of poles for Siberia, Laurentia, and

East Gondwana, which were used in this study analysis, are listed in Table 3. The East Gondwana poles are presented entirely after [35]. Apart from the data published in [35], the pole sequence for Laurentia also included the data for the time interval of 1100–980 Ma obtained by averaging the poles from a recent publication by Weil *et al.* [42]. The Siberian pole sequence consists of the Riphean poles for the Uchur–Maya area [10, 11], a Vendian pole after Gurevich [referred to in 39], and the Early–Middle Cambrian poles from a publication by Pisarevsky *et al.* [33].

The problem of choosing the polarity of paleomagnetic directions for Laurentia, East Gondwana, and Siberia was iteratively discussed in literature [10, 11, 13, 25, 31, 37, 38]. The importance of this issue for paleogeographic and paleotectonic reconstructions is evident, since the chosen polarity determines whether the study craton was located in the Southern or Northern Hemisphere during the reviewed period of time. The essence of the problem consists in that, owing to considerable gaps in the currently available apparent polar wander paths, there are certain doubts about the validity of the polarity options presently adopted by most geoscientists.

We demonstrated earlier [11] that the paleomagnetic data available for Siberia and Laurentia for the 1020–1100 Ma time interval can be matched within a framework of a single supercontinent only in the case when the generally accepted polarity options of the Late Proterozoic paleomagnetic directions are revised either for Laurentia or for Siberia. The result we obtained supports this conclusion. Indeed, one can see in Fig. 5, A that, if we agree with the polarity option accepted by

Table 4. Eulerian poles

No.	Rotation	Φ	Λ	Angle of rotation	Reference
1	Siberia relative to Laurentia	78°	111°	148°	This paper
2	East Gondwana relative to Laurentia	-56°	339°	-166°	[35]
3	Antarctica relative to India	-4.22°	17.14°	92.45°	[34]
4	Australia relative to India	-14.79°	15.35°	64.75°	[34]

Note: The reconstruction of the relative positions of Siberia, Laurentia, and East Gondwana was performed by rotating Siberia and East Gondwana around Eulerian poles 1 and 2. The reconstruction of East Gondwana was performed by rotating Australia and Antarctica around Eulerian poles 3 and 4. See notes for Table 3.

many geoscientists [35, 40, 42] (option 1 in Table 3), then, based on the data listed in the table we should have to place Laurentia and Siberia into different hemispheres at the end of the Late Proterozoic (1050–1100 Ma). Moreover, we should have to subsequently accept that, at least up to 940–1000 Ma ago, their motions were not concordant and, what is more, they moved in opposite directions (Fig. 5a). Conversely, a revision of the paleomagnetic direction polarity choice either for Siberia (Table 3, option 3) or for Laurentia (Table 3, option 2) would, first, provide a concordant motion of these cratons during the time interval of 1050–1100 to 940–1000 Ma ago (Fig. 5b) and, secondly, would allow their amalgamation in the configuration that was suggested by Rainbird *et al.* [36], regardless of paleomagnetic data (Fig. 5c).

We prefer to change the polarity of the Late Precambrian paleomagnetic directions for Laurentia, because a considerable amount of data has been accumulated by now [19, 31, 37, 38] in support of this choice. Proceed-

ing from this choice of the polarity, we can compare the apparent polar wander paths for Siberia, Laurentia, and East Gondwana after matching the respective cratons within a single supercontinent. We retain the relative position of Laurentia and East Gondwana as was inferred in [22, 26, 30, 35] and match Siberia with Laurentia in the manner that we suggested earlier, based on data for the Malga Formation and the Lakhanda Group [10, 11, 25]. Note that the data for the Ui Group confirm the possibility of these mutual positions of Siberia and Laurentia (Fig. 6).

Figure 6 A demonstrates the matching of the East Gondwana cratonic blocks and Siberia with Laurentia, which is shown in its present-day position. The corresponding rotation poles are presented in Table 4. One can see in Fig. 6, B that the paleomagnetic poles of Laurentia, Siberia, and Gondwana for the time interval of 1050–1100 to 940–1000 Ma ago fall into the same region of the Earth, the corresponding segments of the apparent polar wander paths for Siberia and Laurentia almost ideally repeating one another. Thus, the paleomagnetic data available for Laurentia, East Gondwana, and Siberia support unambiguously (keeping in mind the above statement on the polarity choice) the hypothesis on the existence of the Late Proterozoic Rodinia supercontinent. It should be noted, however, that judging from our data, Siberia must have been accreted to the northern regions of Laurentia not by its northern side, as it was assumed in the reconstructions by Dalziel, Hoffman, and others [21, 22, 25, 32, 40], but by its southern and southeastern sides, as suggested by Rainbird *et al.* [36].

The relative positions of Siberia, Laurentia, and East Gondwana 1000–1020 Ma ago are shown in Fig. 7. This reconstruction was made on the assumption that the poles listed in Table 3 had a configuration of option 2, i.e., with a change in the polarity of the paleomagnetic directions for Laurentia and East Gondwana and no changes in the polarity for Siberia. At the same time, we can not completely rule out the probability that a need for changing the polarity for Siberia and not for Laurentia will arise as new data are accumulated (in particular, for the latest Riphean and Early Vendian of Siberia). In this case, the relative positions of the cratons shown in Fig. 7 will not change, except for a symmetric reflection of this reconstruction relative to the equator.

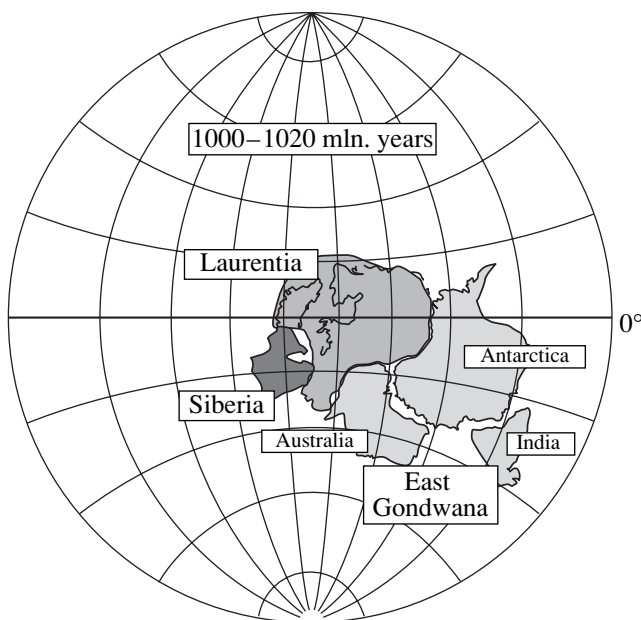


Fig. 7. Reconstruction of the geographic positions of Siberia, Laurentia, and East Gondwana for the time of 1000–1020 Ma ago.

ACKNOWLEDGMENTS

This study was initiated to a considerable degree thanks to extremely fruitful discussions with Prokop'ev (Yakutian Institute of Geology), which lasted several days in August 1986 while waiting for a plane at the Ust'-Maya airport. Later, Prokop'ev gave us a reconnaissance collection of the samples of Late Proterozoic sills and Kandyk Fm. rocks from the Yudoma River valley. Our study of these samples confirmed the value of these objects for paleomagnetic study. We thank the Management of the Paris Institute of Physics of the Earth for the opportunity to perform thermal magnetic cleaning of the samples using the equipment of the Institute's Paleomagnetic Research Laboratory. We are grateful to Enkin (Geological Survey of Canada), who gave us his paleomagnetic software package, and to Semikhatov for numerous fruitful discussions. The reconstructions of the paleogeographic positions of Laurentia, Siberia, and East Gondwana cratonic blocks were performed using the GMAP program created by Torsvik and Smethurst.

This work was supported by the Russian Foundation for Basic Research, project nos. 98-05-65082 and 99-05-64054.

REFERENCES

- Alekseev, V.R. and Kaminskii, F.V., Late Riphean Trapp Magmatism Events in the east of the Aldan Shield, *Sov. Geol.*, 1971, no. 8, pp. 164–167.
- Vasil'ev, I.M., Ovchinnikov, G.V., Semikhatov, M.A., Gorokhov, I.M., Kuznetsov, A.B., Kaurova, O.K., Gorokhovskii, B.M., and Podkovyrov, V.N., The Pb–Pb Age of the Malga Limestone from the Mid–Riphean Kerpil Group in East Siberia. Abstracts of Papers, *I Rossiyskaya konferentsiya po izotopnoi geokhologii. Izotopnoe datirovanie geologicheskikh protsessov: Nove metody i rezul'taty* (Isotopic Dating of Geologic Processes: New Methods and Results), Moscow: GEOS, 2000.
- Gapeev, A.K. and Tsel'movich, V.A., Microstructure of Natural Heterophaseoxidized Titanomagnetite, *Isv. Akad. Nauk SSSR, Fiz. Zemli*, 1986, no. 4, pp. 100–104.
- Gapeev, A.K. and Tsel'movich, V.A., *Stadii okisleniya titanomagnetitovykh zeren v izverzhennykh porodakh* (Stages of Titanomagnetite Grain Oxidation in Eruptive Rocks), Available from VINITI, Moscow, 1988, 1989, no. 1331–B89.
- Zhuravlev, D.Z., Pukhtel', I.S., and Samsonov, A.V., Sm–Nd Ages and Geochemistry of Metavolcanics from the Olonda Greenstone Belt (Aldan Shield), *Izv. Akad. Nauk SSSR, Ser. Geol.*, 1989, no. 2, pp. 39–49.
- Ilyukhin, L.N. and Gudzenko, V.T., Lithology, Mineralogy, and Postsedimentary Reconstruction of Late Proterozoic Rocks in Southwestern Siberian Craton, in *Litologiya i osadochnaya geologiya dokembriya* (Lithology and Sedimentary Geology of the Precambrian), Moscow: Acad. Nauk. SSSR, 1973, pp. 91–93.
- Pavlov, V.E., Nature of the Magnetism of the Bituminous Riphean Rocks in the Uchur–Maya Area, in *Tonkaya struktura geomagnitnogo polya* (Fine Structure of Geomagnetic Field), Moscow: Inst. Fiz. Zemli, Akad. Nauk. SSSR, 1986, pp. 171–180.
- Pavlov, V.E., Estimation of the Possible Movements of the Maya Plate and Yudoma–Maya Block-Fold Area, in *Paleomagnetizm i akkretionnaya tektonika* (Paleomagnetism and Accretionary Tectonics), Leningrad: Vses. Nauchno-Issled. Geologorazved. Inst., 1988, pp. 100–104.
- Pavlov, V.E., Burakov, K.S., Zhuravlev, D.Z., and Tsel'movich, V.A., Paleomagnetism of Sills in the Uchur–Maya Area: Estimation of Late Riphean Magnetic Field Intensity, *Fiz. Zemli*, 1992, no. 2, pp. 92–101.
- Pavlov, V.E. and Galle, I., Reconstruction of the Mutual Positions of Siberia and Laurentia in the Latest Mesoproterozoic from Paleomagnetic Data, *Geotektonika*, 1999, no. 6, pp. 16–28.
- Pavlov, V.E., Gallet, Y., and Shatsillo, A.V., Paleomagnetism of the Upper Riphean Lakhanda Group in the Uchur–Maya Area and the Hypothesis of a Late Proterozoic Supercontinent, *Fiz. Zemli*, 2000, no. 8, pp. 23–34.
- Pushcharovskii, Yu.M., *Vvedenie v tektoniku Tikhookeanskogo segmenta Zemli* (Introduction to the Tectonics of the Pacific Segment of the Earth), Moscow: Nauka, 1972, (Tr. Geol. Inst. Akad. Nauk. SSSR, issue 243).
- Rodionov, V.P., Late Precambrian and Early Paleozoic Paleomagnetism in the Udzha River Area, in *Paleomagnitnye metody v stratigrafii* (Paleomagnetic Methods in Stratigraphy), Leningrad: Vses. Geol. Inst., 1984, pp. 18–28.
- Semikhatov, M.A. and Serebryakov, S.N., *Sibirskii gipostatotip rifeya* (The Riphean Hypostatotype of Siberia), Moscow: Nauka, 1983.
- Stavtsev, A.L., Formation Mechanism of Folds and Faults in the Southern Verkhoyansk Region, *Dokl. Akad. Nauk SSSR*, 1971, vol. 200, no. 6, pp. 1411–1414.
- Stavtsev, A.L., Tectonics and Metallogeny of Marginal Imbricate–Thrust Zones in Ancient Craton Margins, *Geol. Rudn. Mestorozhd.*, 1976, vol. 18, no. 1, pp. 29–45.
- Khramov, A.N., Goncharov, G.I., Komissarova, R.A., Pisarevskii, V.V., and Gurevich, E.M., *Paleomagnitologiya* (Paleomagnetology), Leningrad: Nedra, 1982, p. 312.
- Shanin, L.L., Arakelyants, M.M., Pupyrev, Yu.G., and Kolesnikov, A.G., A new Metallic K–Ar Dating Device, *Mass-spektrometriya i izotopnaya geologiya* (Mass Spectrometry and Isotope Geology), Moscow: Nauka, 1983, pp. 43–50.
- Clark, D.A., New Permian, Silurian, and Devonian Poles from the Lolworth-Ravenswood Block, North Queensland—Implications for the Paleozoic APWP of Gondwana Land, Abstracts of Papers, *8th Scientific Assembly of IAGA with ICMA*, Upsala, 1997, pp. 53–54.
- Collinson, D., *Paleomagnetism*, Cambridge: Cambridge Univ. Press, 1980.
- Condie, K.C. and Rosen, O.M., Laurentia–Siberia Connection Revisited, *Geology*, 1994, vol. 22, pp. 168–170.
- Dalziel, I.W.D., Pacific Margins of Laurentia and East Antarctica–Australia as a Conjugate Rift Pair: Evidence and Implications for an Eocambrian Supercontinent, *Geology*, 1991, vol. 19, pp. 598–601.
- Enkin, R.J., *A Computer Program Package for Analysis and Presentation of Paleomagnetic Data*, Pacific Geoscience Centre, Geological Survey of Canada, 1994.

24. Fletcher, I.R. and Rosman, K.J.R., Precise Determination of Initial Nd from Sm–Nd Isochron Data, *Geochim. Cosmochim. Acta*, 1982, vol. 46, pp. 72–74.
25. Gallet, Y., Pavlov, V.E., Semikhatov, M.A., and Petrov, P.Yu., Late Mesoproterozoic Magnetostratigraphic Results from Siberia: Paleogeographic Implications and Magnetic Field Behaviour, *J. Geophys. Res.*, 2000, vol. 105, no. 7, pp. 16481–16499.
26. Hoffman, P.F., Did the Break–Out of Laurentia Turn Gondwana Inside–Out?, *Science*, 1991, vol. 252, pp. 1409–1412.
27. Kirschvink, J.L., The Least–Square Line and Plane and the Analysis of Paleomagnetic Data, *Geophys. J. R. Astron. Soc.*, 1980, vol. 62, pp. 699–718.
28. McFadden, P.L., The Combined Analysis of Remagnetization Circles and Direct Observations in Paleomagnetism, *Earth and Planetary Sci. Letters.*, 1988, vol. 87, pp. 53–58.
29. McFadden, P.L. and McElhinny, M., Classification of Reversal Test in Paleomagnetism, *Geophys. J. Int.*, 1990, vol. 103, pp. 725–729.
30. Moores, E.M., Southwest US–East Antarctic (SWEAT) Connection: A hypothesis, *Geology*, 1991, vol. 19, pp. 425–428.
31. Park, J.K., Paleomagnetic Constraints on the Position of Laurentia from Middle Neoproterozoic to Early Cambrian Times, *Precambrian Research*, 1994, vol. 69, pp. 95–112.
32. Pelechaty, S.M., Stratigraphic Evidence for the Siberia–Laurentia Connection and Early Cambrian Rifting, *Geology*, 1996, vol. 24, no. 8, pp. 719–722.
33. Pisarevsky, S.A., Gurevich, E.L., and Khramov, A.N., Paleomagnetism of Lower Cambrian Sediments from the Olenek River Section (Northern Siberia): Paleopoles and the Problem of Magnetic Polarity in the Early Cambrian, *Geophys. J. Int.*, 1997, no. 130, pp. 746–756.
34. Powell, C., Mc, A., Roots, S.R., and Veevers, J.J., Pre-Breakup Continental Extension in East Gondwanaland and the Early Opening of the Eastern Indian Ocean, *Tectonophysics*, 1988, vol. 155, pp. 261–263.
35. Powell, C., Li, Z., McElhinny, M., Meert, J., and Park, J., Paleomagnetic Constraints on Timing the Neoproterozoic Break-up of Rodinia and the Cambrian Formation of Gondwana, *Geology*, 1993, vol. 21, pp. 889–892.
36. Rainbird, R.H., Stern, R.A., Khudoley, A.K., Kropachev, A.P., Heaman, L.M., and Sukhorukov, V.I., U–Pb Geochronology of Riphean Supracrustal Rocks from Southeast Siberia and Its Bearing on the Laurentia–Siberia Connection, *Earth Plan. Sci. Lett.*, 1998, vol. 164, pp. 409–420.
37. Schmidt, P.W. and Clark, D.A., Late Proterozoic and Late Paleozoic Reconstructions: Rodinia to Pangaea, Abstracts of Papers, *8th Scientific Assembly of IAGA with ICMA*, Upsala, 1997, p. 54.
38. Schmidt, P.W. and Morris, W.A., An Alternative View of the Gondwana Paleozoic Apparent Polar Wander Path, *Can. J. Earth Sci.*, 1977, vol. 14, pp. 2674–2678.
39. Smethurst, M.A., Khramov, A.N., and Torsvik, T.H., The Neoproterozoic and Palaeozoic Paleomagnetic Data for the Siberian Platform: from Rodinia to Pangea, *Earth Sci. Rev.*, 1998, v. 43, pp. 1–24.
40. Torsvik, T.H., Smethurst, M.A., Meert, J.G., Van der Voo, R., McKerrow, W.S., Brasier, M.D., Sturt, B.A., and Walderhaug, H.J., Continental Break–Up and Collision in the Neoproterozoic and Paleozoic—A Tale of Baltica and Laurentia *Earth Sci. Rev.*, 1996, v. 40, pp. 229–258.
41. Torsvik, T.H. and Smethurst, M.A., Plate Tectonic Modelling: Virtual Reality with GMAP, *Computers and Geosciences*, 1999, vol. 25, no. 4, pp. 395–402.
42. Weil, A., Van der Voo, R., McNiocal, C., and Meert, J., The Proterozoic Supercontinent Rodinia: Paleomagnetically Derived Reconstructions for 1100 to 800 Ma, *Earth Planet. Sci. Letters.*, 1998, vol. 154, p. 13–24.
43. York, D., Least Squares Fitting of Straight Line, *Can. J. Phys.*, 1996, vol. 44, pp. 1079–1086.
44. Zijderveld, J.D.A., A.C. Demagnetization of Rocks: Analysis of Results, in *Methods in Paleomagnetism*, Collinson, D.W. and Creer, K.M., Eds., Amsterdam: Elsevier, 1967, pp. 254–286.

Reviews: G.Z. Gurarii and V.I. Kovalenko